

Evolution of the geomorphology of erodible bedform submitted to fluid

Z.-C. LIU, W.-J. FAN

*Chongqing Jiaotong University
107#, Dahuang Road, Daping, Yuzhong District
Chongqing, 400074, P.R. China
e-mail: Liuzc17@aliyun.com*

A COUPLED MAP LATTICE (CML) MODEL was developed to study the evolution of desert's geomorphology. The numerical results show that the model presents abundant spatiotemporal patterns. In spatial behaviors, the model illustrates the mechanism of both weakly and strongly coupled systems. In temporal behaviors, the model illustrates the stochastic effects. The model is able to demonstrate the physically layered coupling mechanism and shows the initiative and driven coupled systems. The evolutionary processes of the model are also analyzed with physical geomorphological laws. The desert's geomorphologic forms, such as sand ripples and dunes, result from the combined actions of deterministic and stochastic effects. Verified by the field data, this study qualitatively illustrates the geomorphologic evolution of desert. Moreover, the model is applicable to the evolution of ripples and dunes with loose sand caused by water currents on fluvial beds, e.g., river beds in the lower reaches of the Yellow River, China.

Copyright © 2014 by IPPT PAN

1. Introduction

THE GEOMORPHOLOGIC EVOLUTION OF DESERT is a complicated process [1–13]. The formation of dunes and ripples is still not well-understood. For the earth, the external energy input is primarily coming from the sun. For a particular region, the dynamic factors to create the change of surface geomorphology are mainly climate, hydrology, earth crust movement and human activities, all leading to various landforms. Due to the intrinsic randomness of the region's evolution caused by the nonlinear coupling interactions among affecting factors, it may be impossible to forecast the future evaluation of a geomorphologic form in a specific region precisely on the basis of its present state, though the final evolutionary result can be recognized. The desert's geomorphology results from various stochastic and deterministic mechanisms, including multi-scale and wind-blown sand flows, fluid-solid interaction, meteorology and hydrology. In present work, we will address the evolution of the geomorphology of erodible bedform submitted to fluid. For convenience, sediments are supposed to be non-cohesive and uniform with the particle size within 0.5–50 mm herein in this paper.

In the last decade, there has been much interest in the study of the large assemblies of chaotic elements that can spontaneously evolve to a state of large-scale synchronization and form different patterns. In these studies, a convenient tool of analyzing the characteristics of spatiotemporal system is the coupled map lattice (CML) model [14], which is applicable to a discrete-space and discrete-time system of interacting elements with states varying continuously according to specific functions. For more details of the CML model, see references [15–19]. The early results were comprehensively described by CROSS and HOHENBERG [15], while recent representative methods and suggestions for future work about synchronization phenomena were reviewed by ACEBRON *et al.* [16]. Some results about patterns can be found in [17]. These studies may provide a new way of describing the geomorphologic evolution submitted to a fluid flow [20–25].

The general form of CML model is expressed as follows:

$$(1.1) \quad x_{(n+1)}(i) = (1 - \varepsilon)f(x_n(i)) + \frac{\varepsilon}{2}[f(x_n(i-1)) + f(x_n(i+1))] + p_n(i),$$

where n = discrete time step, i = discrete lattice with periodical spatial boundary, $f(x)$ = logistic map or other forms of map (here the logistic map and the tent map), and $p_n(i)$ = local or global coupling. Normally, the model is based on the one-dimensional (1D) diffusion mechanism. To describe diffusion in the framework of CML model, considering the interaction between fluid flow and sediment [26–30], this paper is to expand the methods used in 1D cases to 2D ones, and rebuild them as to model the geomorphologic evolution of desert. The model developed in this paper is able to describe: 1) the interaction among many physical factors, 2) stochastic effects and 3) strongly and weakly coupled system functions.

The multi-scale description of CML model for formation of the bedform is proposed. Here, the interior region of a desert is taken as a major application of the model. Formation of the aeolian ripples is thought to be a result of wind action on loose sand. Starting from a flat bed, three regimes are identified: appearance of an initial wavelength, coarsening of the pattern, i.e., a progressive increase of typical length scale with time and saturation of the ripples. The main focus is a general picture of the model's dynamic characteristics in describing topographies and revealing their formation process. A schematic sketch of the evolutionary process is investigated with numerical results.

2. Geomorphologic system as a dissipative structure

It has been recently realized that the geomorphologic evolution is a dissipative structure [31–33]. For a specific desert region, the driving dynamic factors in changing geomorphology are climate, hydrology and human activity, of which wind is the most active. In spite of the asynchrony occurring occasionally between

geomorphology and the dynamic factors due to the crust sudden violent movements, the geomorphologic evolution corresponds approximately synchronously to these dynamic factors on the scale of long time and wide space. An important aspect of a geographical region is substance cycle and energy flow. With no consideration of chemical reaction, the change of a substance in an approximately close geographical region can be formulated as

$$(2.1) \quad \frac{\partial \rho}{\partial t} + \text{div}(\rho \vec{u}) = q,$$

where ρ is the density of the substance, \vec{u} is velocity, q is the increasing rate at unit's time and volume. In some systems, variable A may be decomposed as

$$(2.2) \quad A = \text{constant component} + \text{trend component} \\ + \text{periodic component} + \text{random component} + \text{mutant component},$$

where the constant component can be regarded as the average value of A . The trend component means relatively stable part of A , and the mutant component means suddenly changing part of A . Obviously, the timescale corresponding to each component is usually different.

There are two evolutionary processes in a region: 1) from order to disorder and 2) from disorder to order. The corresponding energy fluxes are dissipative and accumulating processes. The entropy fluxes often cause the entropy of a region to increase or decrease. The governing equations of a regional evolutionary process are the maximum entropy principle corresponding to equilibrium state and the minimum entropy production rate principle corresponding to non-equilibrium state [34–37]. The entropy can be calculated as $d\varepsilon = d\varepsilon_i + d\varepsilon_e$, where $d\varepsilon$ is the entropy for a specific region, $d\varepsilon_i$ is internal entropy production and $d\varepsilon_e$ is the environmental entropy flux which contains two parts, the local change caused by unsteady effect and the convective change caused by non-uniform effect.

Movements of both wind-sand and water-sediment are essential interactions between fluid and sediments [38–45]. Sometimes, the lattice Boltzmann method is used to study such a problem [46–47]. In this paper, the coupling interaction of wind and sand is addressed. Wind has an effect on the form of sediment motion, such as incipience, suspending, saltation and bedload transport. Sediment motion also has an effect on wind. Hence, the desert's geomorphology is the function of the local and temporal properties of sediment and wind.

The governing equation of wind is Navier–Stokes (N-S) equation

$$(2.3) \quad \frac{\partial u_i}{\partial t} + u_j \frac{\partial u_i}{\partial x_j} = -\frac{\partial p}{\partial x_i} + \nu \frac{\partial^2 u_i}{\partial x_k \partial x_k}, \quad \frac{\partial u_i}{\partial x_i} = 0,$$

where u_i is the velocity in i direction and ν is the kinematic viscous coefficient. Note that, in the expression above, gravitation is body force and fluid is assumed

to be incompressible. For convenience, the pressure p absorbs body force and the repeated subscript means Einstein's summation convention.

The dynamic processes of wind for forming geomorphologic pattern are mainly by convective and diffusive mechanisms, and the function of precipitation erosion is similar to that of wind. These factors originate the change of aggregation morphology as a function of time. The spatial and temporal distributions of desert geomorphology exhibit randomness and self-similarity in a statistical sense at the same time. The desert's geomorphology shows multiple patterns, such as plane beds, sand-ripples, longitudinal dunes, movable plane beds and sand waves. Surely these patterns are the results of long-term accumulation of interactions among various factors.

Sediment transport and bed deformation caused by fluid flowing, as for single sediment particle [48, 49], can be summarized as follows: incipient starting \rightarrow rolling (occasionally sliding) \rightarrow occasionally rolling and occasionally saltating \rightarrow continuous saltating \rightarrow occasionally saltating and occasionally suspending \rightarrow suspending. The sediment particle often begins to suspend from saltating, which is its basic rising form. The moving forms of large-amount sediment particles can be considered as bed load and suspended load, and both of them can transform into each other because of different magnitude of velocity. The sediment transport connects closely with turbulent coherent structure. The following random factors influence the sediment transport: 1) velocity fluctuation exerting on sediment, 2) irregular shapes of sediment, 3) contingency of location and arrangement of sediments on the bed, 4) inhomogeneity of sediment compounding, 5) transient and uncertain locations between the coarse and fine sediments, 6) complexity of interaction among fine sediment particles and 7) unsteady supply of sediment, etc. Furthermore, in unsteady and non-uniform flow, there is a hysteresis of sediment movement to respond to velocity change. The hysteresis is connected with sediment composition and obviously shows intermittent and paroxysmal properties. The essence to investigate the evolutionary processes of the sand ripples and dunes is to study the properties of the feedback of many coupled factors, such as sediment transport, characters of fluid flowing, sediment supply and initial and boundary conditions, varying with time and space. If sediment concentration is high enough, for aquatic sediment laden flow, it will become hyper-concentrated flow; thus, not only is there a hysteresis of interactions between sediment and flowing, but also the fluid flow belongs to Bingham fluid instead of Newtonian fluid. In 2D case, its constitutive equation reads

$$\tau = \tau_b + \eta \frac{du}{dy},$$

where τ is shear stress, τ_b is Bingham yield stress, η is rigidity coefficient and sometimes it is also called viscous coefficient, du/dy is velocity gradient. The ex-

perimental results show that the Bingham yield stress and the rigidity coefficient are functions of sediment concentration and sediment properties respectively. For low sediment-laden flow and hyper-concentrated flow, sediment transport is influenced by local flowing structure. Existence of sediments has influence on flowing structure to make it different from that of clear flowing case. However, the fact that the coherent structure is made up of turbulent spots remains unchangeable. From the viewpoint of phenomenological mechanism, the incipient motion of sediment particles is ultimately dominated by the turbulent bursting processes, and the sediment transport is influenced by turbulent coherent structure, both of which show chaotic properties in space and time. It is known that, in relatively wide range of Reynolds number, there is a one-to-one correspondence between the sediment transport and the flowing intensity [39].

It is well known that the aeolian ripples are the result of the reptation movement, caused by the collisions of falling particles. On the other hand, the aeolian dunes, many times greater in size than the aeolian ripples, are instabilities formed by the direct action of the wind. When the fluid is water, collisions are dumped and reptation is absent, thus there is no equivalent to the “aeolian ripples” under water. The bed instability under water is influenced directly by the water stream, so that they correspond to the dunes of the aeolian case. However, these forms under water are many times smaller than the aeolian dunes. Although the aeolian ripples generally have the same length-scale as the aquatic ripples, their dynamic properties are different from the aquatic ripples. There are some differences between aeolian bed-load and aquatic bed-load.

Despite this, from the viewpoint of phenomenological process, the field measured geomorphology of aeolian dunes and river bedforms, such as the aquatic ripples and dunes, connects closely with fluid flow’s properties. As for their concrete growing mechanism, though there are few theories developed to apply them, there is no accepted mathematical model based on any of these theories to predict the growing processes. On the assumed conditions of the study, as for both the geomorphology of desert, such as aeolian dunes, and the subaquatic geomorphology of a river, such as aquatic dunes, the common properties of them are as follows: 1) the size, volume and pattern are the results of direct or indirect actions of the fluid flow, the characters of the geomorphology are connected closely with the fluid flow’s properties, 2) the evolutionary processes of geomorphology are the results of combined actions of many stochastic factors without being precisely measured, and they are weaved by the intrinsic deterministic and stochastic factors to show chaotic characters, 3) the driving factors to cause interactions between the fluid–sediment and sediment–sediment can be described in types as the convective mechanism, diffusive mechanism, periodic force and random force, 4) if we neglect the interacting details and only consider the in-

put, output and the final results, then, some concrete developing processes of geomorphology of aeolian and aquatic ripples and dunes can be circumambulated. Although there are differences in growing mechanism, however, common properties still exist between the input and the output. Thus, it is possible to model them in a unified approach.

FRISCH [50] gave a poor man's N-S equation, i.e., $v_{t+1} = 1 - (v_t)^2$ ($t = 1, 2, \dots$), Eq. (3.2) in his book, as a CML model to describe the properties of fully developed turbulence. Some scholars [51–53] thought that, in one-dimensional cases, KdV-Burgers equation,

$$\frac{\partial u}{\partial t} + u \frac{\partial u}{\partial x} - \gamma \frac{\partial^2 u}{\partial x^2} + \beta \frac{\partial^3 u}{\partial x^3} = 0,$$

is a control equation of turbulence. To consider the above results comprehensively, and from the practical viewpoint as a primary approximation, we deem that the proper form of CML model, which contains nonlinear, convective and diffusive mechanisms, can be used to model the evolutionary mechanism of sand ripples and dunes submitted to fluid flow. The following CML model developed in this paper was based on such an assumption.

3. CML models

If we consider the discrete form

$$\frac{u_i^{n+1} - u_i^n}{\Delta t} = \gamma \frac{u_{i+1}^n - 2u_i^n + u_{i-1}^n}{\Delta x^2}$$

of the PDE,

$$\frac{\partial u}{\partial t} - \gamma \frac{\partial^2 u}{\partial x^2} = 0,$$

which describes diffusion phenomenon. Let

$$\frac{\varepsilon}{2} = \frac{\gamma \Delta t}{\Delta x^2},$$

then

$$u_i^{n+1} = (1 - \varepsilon)u_i^n + \frac{\varepsilon}{2}(u_{i+1}^n + u_{i-1}^n),$$

and the method used by KANEKO [14] is adopted, the following model can be developed:

$$(3.1) \quad x_{n+1}(i) = (1 - \varepsilon)f(x_n(i)) + \frac{\varepsilon}{2}[f(x_n(i+1)) + f(x_n(i-1))].$$

If other factors such as open system and feedback are considered, the above model can accommodate another term $p_n(i)$, thus reducing to model (1.1), which has been widely used, where $f(x)$ is logistic map or other form of map. If

$$p_n(i) = (\varepsilon - \varepsilon_1)f(x_n(i)) + \frac{\varepsilon_1}{N} \sum_{i=1}^N f(x_n(i)),$$

then it becomes the model adopted by PINEDA and COSENZA [54]. If $p_n(i) = 0$, then in 2D cases, it becomes the model adopted by FRANCISCO and MURUGANANDAM [55]. Model (3.1) may reflect more physical meanings if other components are added in terms of physical interactions and coupling ways.

The N-S equations have the following form:

$$(3.2) \quad \frac{\partial \varphi}{\partial t} + u_x \frac{\partial \varphi}{\partial x} + u_y \frac{\partial \varphi}{\partial y} = f_x + v \left(\frac{\partial^2 \varphi}{\partial x^2} + \frac{\partial^2 \varphi}{\partial y^2} \right).$$

By a upwind scheme,

$$(3.3) \quad \begin{aligned} & \frac{\varphi_{i,j}^{n+1} - \varphi_{i,j}^n}{\Delta t} + u_{x,i,j}^n \frac{CIE\varphi_{i+1,j}^{n+1} + CIP\varphi_{i,j}^{n+1} - CIW\varphi_{i-1,j}^{n+1}}{\Delta x} \\ & + u_{y,i,j}^n \frac{CJE\varphi_{i,j+1}^{n+1} + CJP\varphi_{i,j}^{n+1} - CJW\varphi_{i,j-1}^{n+1}}{\Delta y} \\ & = f_{xi,j} + v \left(\frac{\varphi_{i+1,j}^{n+1} - 2\varphi_{i,j}^{n+1} + \varphi_{i-1,j}^{n+1}}{(\Delta x)^2} + \frac{\varphi_{i,j+1}^{n+1} - 2\varphi_{i,j}^{n+1} + \varphi_{i,j-1}^{n+1}}{(\Delta y)^2} \right) \end{aligned}$$

Let

$$\frac{\beta_x}{2} = \frac{\Delta t}{\Delta x}, \quad \frac{\beta_y}{2} = \frac{\Delta t}{\Delta y}, \quad \frac{\varepsilon_x}{2} = \frac{v\Delta t}{(\Delta x)^2}, \quad \frac{\varepsilon_y}{2} = \frac{v\Delta t}{(\Delta y)^2},$$

then we can obtain the following schemes:

when $i = 1$,

$$\begin{aligned} & \left\{ 1 + f_x(\varphi_{i,j}^n) \times \frac{\beta_x}{2} \times CIP + f_y(\varphi_{i,j}^n) \times \frac{\beta_y}{2} \times CJP + \varepsilon_x + \varepsilon_y \right\} \varphi_{i,j}^{n+1} \\ & + \left[f_x(\varphi_{i,j}^n) \times \frac{\beta_x}{2} \times CIE - \frac{\varepsilon_x}{2} \right] \varphi_{i+1,j}^{n+1} + \left[f_y(\varphi_{i,j}^n) \times \frac{\beta_y}{2} \times CJE - \frac{\varepsilon_y}{2} \right] \varphi_{i,j+1}^{n+1} \\ & - \left[f_y(\varphi_{i,j}^n) \times \frac{\beta_y}{2} \times CJW + \frac{\varepsilon_y}{2} \right] \varphi_{i,j-1}^{n+1} \\ & = f_{xi,j} \times \Delta t + \varphi_{i,j}^n + \left[f_x(\varphi_{i,j}^n) \times \frac{\beta_x}{2} \times CIW + \frac{\varepsilon_x}{2} \right] f(\varphi_{NI,j}^n); \end{aligned}$$

when $j = 1$,

$$\begin{aligned} & \left\{ 1 + f_x(\varphi_{i,j}^n) \times \frac{\beta_x}{2} \times CIP + f_y(\varphi_{i,j}^n) \times \frac{\beta_y}{2} \times CJP + \varepsilon_x + \varepsilon_y \right\} \varphi_{i,j}^{n+1} \\ & + \left[f_x(\varphi_{i,j}^n) \times \frac{\beta_x}{2} \times CIE - \frac{\varepsilon_x}{2} \right] \varphi_{i+1,j}^{n+1} - \left[f_x(\varphi_{i,j}^n) \times \frac{\beta_x}{2} \times CIW + \frac{\varepsilon_x}{2} \right] \varphi_{i-1,j}^{n+1} \\ & + \left[f_y(\varphi_{i,j}^n) \times \frac{\beta_y}{2} \times CJE - \frac{\varepsilon_y}{2} \right] \varphi_{i,j+1}^{n+1} \\ & = f_{xi,j} \times \Delta t + \varphi_{i,j}^n + \left[f_y(\varphi_{i,j}^n) \times \frac{\beta_y}{2} \times CJW + \frac{\varepsilon_y}{2} \right] f(\varphi_{i,NJ}^n); \end{aligned}$$

when $i = NI$,

$$\begin{aligned} (3.4) \quad & \left\{ 1 + f_x(\varphi_{i,j}^n) \times \frac{\beta_x}{2} \times CIP + f_y(\varphi_{i,j}^n) \times \frac{\beta_y}{2} \times CJP + \varepsilon_x + \varepsilon_y \right\} \varphi_{i,j}^{n+1} \\ & - \left[f_x(\varphi_{i,j}^n) \times \frac{\beta_x}{2} \times CIW + \frac{\varepsilon_x}{2} \right] \varphi_{i-1,j}^{n+1} + \left[f_y(\varphi_{i,j}^n) \times \frac{\beta_y}{2} \times CJE - \frac{\varepsilon_y}{2} \right] \varphi_{i,j+1}^{n+1} \\ & - \left[f_y(\varphi_{i,j}^n) \times \frac{\beta_y}{2} \times CJW + \frac{\varepsilon_y}{2} \right] \varphi_{i,j-1}^{n+1} \\ & = f_{xi,j} \times \Delta t + \varphi_{i,j}^n - \left[f_x(\varphi_{i,j}^n) \times \frac{\beta_x}{2} \times CIE - \frac{\varepsilon_x}{2} \right] f(\varphi_{1,j}^n); \end{aligned}$$

when $j = NJ$,

$$\begin{aligned} & \left\{ 1 + f_x(\varphi_{i,j}^n) \times \frac{\beta_x}{2} \times CIP + f_y(\varphi_{i,j}^n) \times \frac{\beta_y}{2} \times CJP + \varepsilon_x + \varepsilon_y \right\} \varphi_{i,j}^{n+1} \\ & + \left[f_x(\varphi_{i,j}^n) \times \frac{\beta_x}{2} \times CIE - \frac{\varepsilon_x}{2} \right] \varphi_{i+1,j}^{n+1} - \left[f_x(\varphi_{i,j}^n) \times \frac{\beta_x}{2} \times CIW + \frac{\varepsilon_x}{2} \right] \varphi_{i-1,j}^{n+1} \\ & - \left[f_y(\varphi_{i,j}^n) \times \frac{\beta_y}{2} \times CJW + \frac{\varepsilon_y}{2} \right] \varphi_{i,j-1}^{n+1} \\ & = f_{xi,j} \times \Delta t + \varphi_{i,j}^n - \left[f_y(\varphi_{i,j}^n) \times \frac{\beta_y}{2} \times CJE - \frac{\varepsilon_y}{2} \right] f(\varphi_{i,1}^n); \end{aligned}$$

when $1 < i < NI, 1 < j < NJ$,

$$\begin{aligned} & \left\{ 1 + f_x(\varphi_{i,j}^n) \times \frac{\beta_x}{2} \times CIP + f_y(\varphi_{i,j}^n) \times \frac{\beta_y}{2} \times CJP + \varepsilon_x + \varepsilon_y \right\} \varphi_{i,j}^{n+1} \\ & + \left[f_x(\varphi_{i,j}^n) \times \frac{\beta_x}{2} \times CIE - \frac{\varepsilon_x}{2} \right] \varphi_{i+1,j}^{n+1} - \left[f_x(\varphi_{i,j}^n) \times \frac{\beta_x}{2} \times CIW + \frac{\varepsilon_x}{2} \right] \varphi_{i-1,j}^{n+1} \\ & + \left[f_y(\varphi_{i,j}^n) \times \frac{\beta_y}{2} \times CJE - \frac{\varepsilon_y}{2} \right] \varphi_{i,j+1}^{n+1} - \left[f_y(\varphi_{i,j}^n) \times \frac{\beta_y}{2} \times CJW + \frac{\varepsilon_y}{2} \right] \varphi_{i,j-1}^{n+1} \end{aligned}$$

$$= f\left(\frac{1}{NI \times NJ} \sum_{i=1}^{NI} \sum_{j=1}^{NJ} \varphi_{i,j}^n\right) + \varphi_{i,j}^n + \frac{1}{4} \left\{ \sum_{-1 \leq i,j \leq 1} \xi(n) f(\varphi_{i,j}^n - \varphi_{i-ij,j-ji}^n) * \cos(\varphi_{i,j}^n - \varphi_{i-ij,j-ji}^n) \right\},$$

where $\xi(n)$ is a random number uniformly distributed within $(0, 1)$, $f_x(x)$ and $f_y(y)$ take the logistic and tent map forms, respectively,

$$\begin{aligned} CIE &= [[\text{sgn}(-f_x(\varphi_{i,j}^n)), 0]], \\ CIP &= \text{sgn}(f_x(\varphi_{i,j}^n)), \\ CIW &= [[\text{sgn}(f_x(\varphi_{i,j}^n)), 0]], \\ CJE &= [[\text{sgn}(-f_y(\varphi_{i,j}^n)), 0]], \\ CJP &= \text{sgn}(f_y(\varphi_{i,j}^n)), \\ CJW &= [[\text{sgn}(f_y(\varphi_{i,j}^n)), 0]], \end{aligned}$$

and $[[a, b]]$ means to take the larger value of a and b . The logistic map is

$$(3.5) \quad f(x) = 1 - ax^2, \quad a \in [0, 2], \quad x \in [-1, 1], \quad f(x) \in [-1, 1].$$

The tent map is

$$(3.6) \quad f(x) = \begin{cases} -2 - 2x, & x \in [-1, -0.5), \\ 2x, & x \in [-0.5, 0.5), \\ 2 - 2x, & x \in [0.5, 1]. \end{cases} \quad f(x) \in [-1, 1].$$

Let

$$(3.7) \quad P(n) = \frac{1}{(NI \times NJ)} \sum_{i=1}^{NI} \sum_{j=1}^{NJ} (\varphi_{i,j}^n),$$

where i and j mean step distances in x and y directions, respectively. With the final value $\varphi_{i,j0}$, the following transformation procedure applies:

$$(3.8) \quad \varphi_{i,j} = \varphi_{i,j0} + \varphi_{i,j_s},$$

where φ_{i,j_s} is a Gaussian normal random variable. Hence, the expected value and standard deviation are written as follows:

$$(3.9) \quad E(\varphi_{i,j_s}) = \lambda_{ex} \left(\frac{1}{NI \times NJ} \sum_{i=1}^{NI} \sum_{j0=1}^{NJ} \varphi_{i,j0} \right),$$

$$(3.10) \quad D(\varphi_{i,j_s}) = \lambda_{dx} \sqrt{\frac{1}{NI \times NJ - 1} \sum_{i=1}^{NI} \sum_{j_0=1}^{NJ} (\varphi_{i,j_0}(k) - E(\varphi_{i,j_0}))^2}.$$

Here, let $\lambda_{ex} = 0.7$, and $\lambda_{dx} = 0.1$. The value of entropy can be calculated as

$$(3.11) \quad S_p = - \sum_{i,j} Q(i,j) \lg Q(i,j),$$

where $Q(i,j)$ is the probability of spatial point $\varphi_{i,j}$ falling into the range (i_0, j_0) . The boundary condition will be periodic, and the initialization takes random values. The modelling results are presented in the following section.

4. Numerical results

Many sets of numerical experiment show that all experimental results follow the same law, and part of results is herein presented. In the numerical experiments, $(\beta_x, \beta_y, \varepsilon_x, \varepsilon_y) = (0.23, 0.22, 3.1, 3.1)$, $NI = 238$ and $NJ = 223$. Here NI and NJ are system sizes in x and y directions, respectively. Numerical results show that if NI and NJ take other values, such as $(120, 130)$ or $(345, 457)$, the essential evolutionary laws are identical. Part of the initial 1000 steps is ignored, because numerical results show that, after certain steps, the essential evolutionary laws are identical. Figure 1 shows $U-I-J$ at the final step, Fig. 2 does $U-I$ at the final 100 steps with $J = 50$ and without the transformation by Eq. (3.8), Fig. 3 does $U-J$ at the final step with $I = 50$ without transformation, and Fig. 4 does $P(n-1)-P(n)$ at final 100 iterative steps.

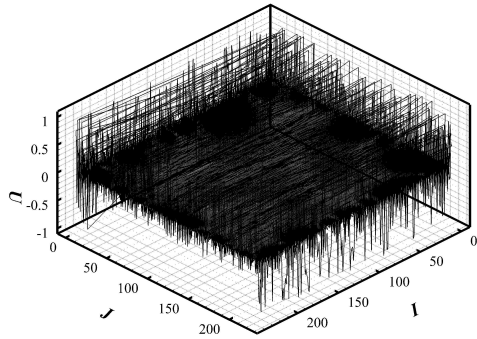


Fig. 1. $U-I-J$ diagram.

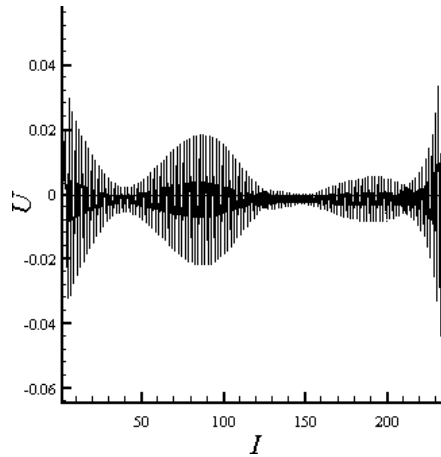


Fig. 2. $U-I$ curve.

Figures 5–8 show the results for $(\beta_x, \beta_y, \varepsilon_x, \varepsilon_y) = (0.25, 0.31, 3.1, 3.1)$.

Figures 9–12 show the results for $(\beta_x, \beta_y, \varepsilon_x, \varepsilon_y) = (0.95, 0.71, 0.04, 0.03)$.

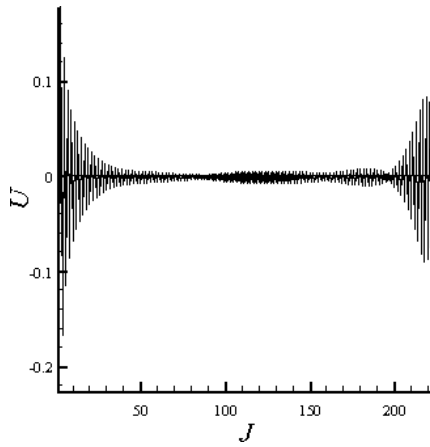


Fig. 3. U - J curve.

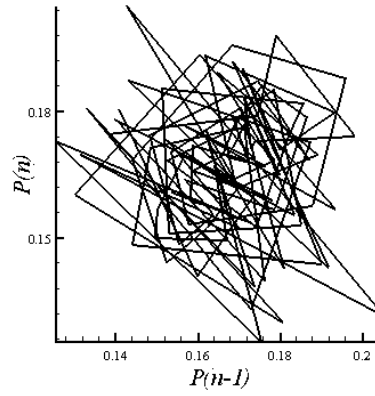


Fig. 4. $P(n - 1)$ - $P(n)$ curve.

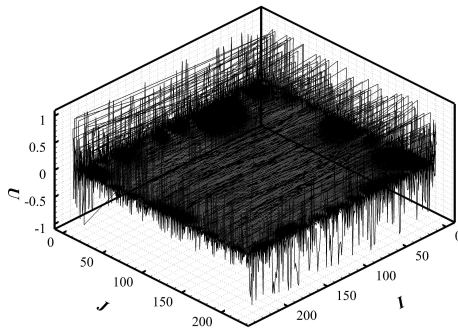


Fig. 5. Relation of U - I - J .

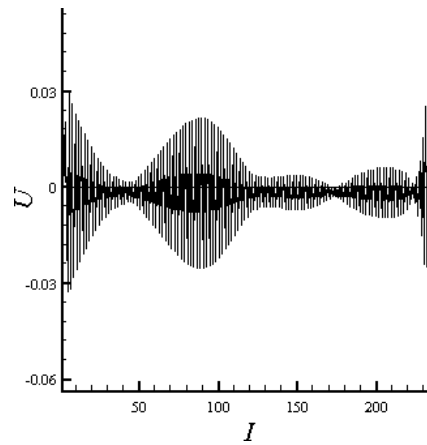


Fig. 6. Relation of U - I .

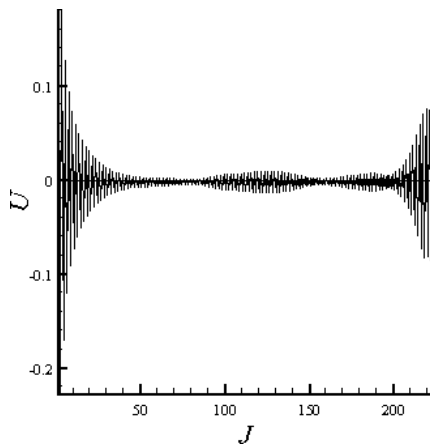


Fig. 7. Relation of U - J .

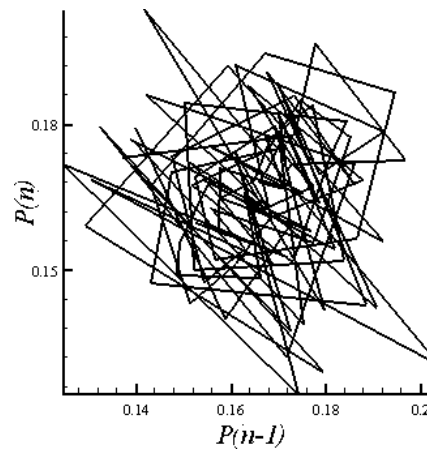


Fig. 8. Relation of $P(n - 1)$ - $P(n)$.

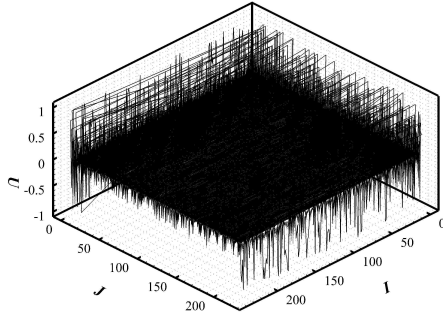


Fig. 9. Variation of U with I and J .

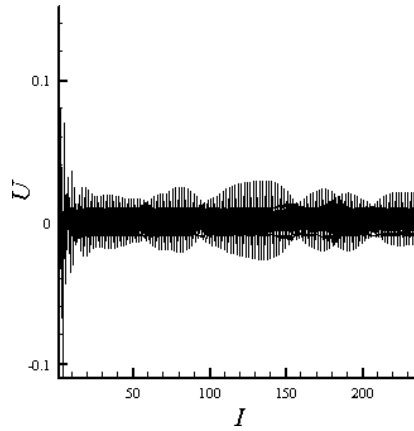


Fig. 10. Variation of U with I .

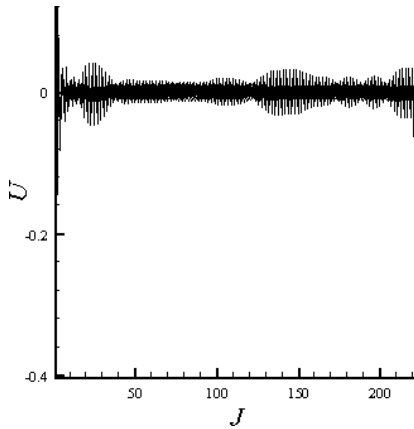


Fig. 11. Variation of U with J .

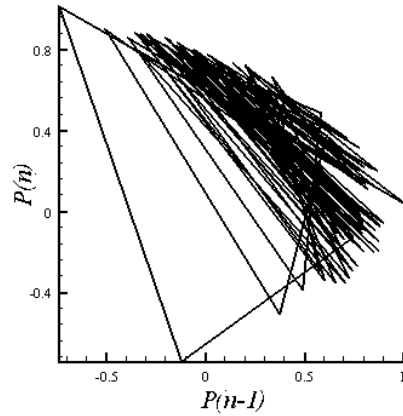


Fig. 12. Variation of $P(n - 1)$ with $P(n)$.

The values of entropy are provided in Table 1. However if the final calculated results are transformed with Eq. (3.8), S_P will become 0.0.

Table 1. Relationship between S_P and $(\beta_x, \beta_y, \varepsilon_x, \varepsilon_y)$.

Set	Set 1	Set 2	Set 3
Value	0.23, 0.22, 3.1, 3.1	0.25, 0.31, 3.1, 3.1	0.95, 0.71, 0.04, 0.03
S_P	4.8397	4.8316	4.5774

5. Structure of the model and characteristics of desert's geomorphology

The numerical results have shown that increases of β_x and β_y make the patterns chaotic, and increases of ε_x and ε_y make the patterns ordered. Here, the order means that the value of entropy S_P becomes small.

Relations between the whole properties of the model and the local coupling forms are that the whole properties of the model connect more closely (whether the local coupling form is being non-linear or not) than their concrete forms. The local properties of the model connect closely with the non-linear coupled map's concrete form. The local pattern and the whole pattern of the system show the phenomenon of hologram in a relatively large specific zone, as a phenomenon of pattern on tiger furs.

For an isolated system, all the components of the system can spontaneously tend to be uniform and finally become an equilibrium state, and then the entropy of the system becomes maximum. However, in the real world, it is obvious that the regional physiognomy shows various landforms. As the diversity of desert geomorphology in different regions is caused by different evolutionary driving forces, the diversity of desert geomorphology in a region results from the non-linear evolutionary mechanism. For a natural physiognomy evolution system, it is the evolutionary non-equilibrium to produce the diversity of landforms to enhance the system stability. The self-organization evolutionary mechanism makes the system show some self-repairing ability, i.e., the function of the system to recover its original state after being slightly disturbed. The evolutionary mechanism and process of co-existence of order and disorder, determinability and randomness, maintain the geographical region in a relatively stable evolutionary state. Results of the numerical simulation illustrate that the patterns of the desert geomorphology are the deterministic evolutionary results of the stochastic evolutionary processes and the interactions between the deterministic and stochastic movements. If the evolutionary timescale is long enough, and only if the exterior natural conditions are similar, the final evolutionary landform features of a desert region are also similar in the case of being disturbed suddenly. In other words, in the geological timescale, the desert landform features are independent of its initial conditions. Under the conditions of the same geographical environments, the evolutionary patterns of the identical region in different periods can have the similar statistical results as those from different regions under the same period. The final evolutionary landform of a region shows self-resemble to some extent anytime and anywhere. This may be the physical basis for the application of fractal theory to the landform study [10–11], [20–25], [56]. The field snapshots of the desert landform features taken by man-made satellites also support this fact. To improve the model so that it provides a quantitative comparison between the modelling result and the field survey is the next issue to address.

Based on the former discussion and considering the comparison relations between evolution of the geomorphology submitted to water and air, we could conclude that the evolutionary process of the bed morphology made up of uncohesive sand particles under the water surface of fluvial rivers [57–58], e.g., the

bed morphology in some places of the middle and the lower reaches of the Yellow River, has similar properties as described above.

6. Evolutional processes of dunes and ripples

It has long been recognized that the formation and growth of aeolian bedform is related to the phase lag between sediment transport and bed elevation. If the evolution of a flat sand bed is dominated by a turbulent shear flow, the sediment transport saturation length, which is the length needed for the sand flux to adapt to a change in wind strength, controls a dune developing process. The different modes of sediment transport by the fluid in different situations can lead to different bedform instabilities. For small enough aeolian dunes, the slip face instability is washed out by the saturation transients. The experiments show that the formation of dunes follows the mechanism of a nonlinear pattern coarsening. Thus, the dunes cannot be formed by a linear, but nonlinear instability mechanism. The numerical results of the CML model lead one to conclude once again that both aeolian and subaqueous dunes result from the nonlinear instability of a flat bed, instead of the linear instability mentioned before.

Aeolian ripples are generated by a screening instability: the upwind face (windward or stoss slope) of ripples receives more impacts of saltating grains than the downwind face (the lee slope). After the linear stage during which the ripples emerge, they exhibit a pattern coarsening by progressive merging of bedforms. As the ripples grow, nonlinear effects become important, ripples become asymmetric, with the downwind slope slightly steeper than the upwind slope, merging processes take place and the ripple wavelength increases. The ripple pattern initially develops dislocations (which are sometimes called “terminations” and “antiterminations” which move laterally along the ripple crests). In well-developed ripple fields, the crests display bifurcation and defects (Y junctions), which show the formation of ripples by a linear instability and due to merging events. The numerical results of the CML model show that the aeolian ripples and aeolian dunes connect with two different linear instabilities, so do the aquatic ripples and aquatic dunes. For the heterogeneous situation, the cases remain the same besides that the forming evolutional processes become complicated.

Moreover, the analysis of the numerical results of the CML model leads us to argue that:

- 1) The reason that there is a scaling law for aeolian dunes on Mars, Venus, Earth, and for subaqueous ripples [59–61] results from a common interacting mechanism between the particles and the fluid. For in an unsteady, non-uniform, non-equilibrium and instable state, there should exist some hierarchical scaling laws, although their forms may be changeable and complicated. However, in any time, their statistic average forms are definite.

2) The existing solitary phenomena in mutual actions among the aeolian sand dunes results from the nonlinear mechanism, its physical mechanism is essentially same as that of interactions among isolated water waves, first founded by John Scott Russell in 1834, as both of them are caused by fluid flow.

3) The aeolian ripples and aquatic ripples are mainly controlled by the small vortexes, but aeolian dunes and aquatic dunes are ruled by the coherent structure. The profile between aeolian ripple and aeolian dune, and that between aquatic ripple and the aquatic dune, shares some features of the coherent structure of turbulent flow between the boundary layer and the outer flowing region.

Based on the numerical results of the CML model, to our knowledge, we made some new predictions as follows to be verified by the experiments: 1) in the specific conditions, the solitary phenomena can also exist in aquatic dunes. In the field of the fully developed aeolian dune, there exist some hierarchical scaling laws of the wave length; 2) although the aeolian ripples are formed by linear instability from the viewpoint of phenomenological analysis, we think that the nonlinear mechanism plays an important role in the actual physical mechanism of the aeolian ripple evolutionary processes, just like the case of sub-layer structures in boundary layer of fluid flow.

7. Concluding remarks

Based on a CML model for 1D diffusive process, a CML model for 2D diffusive and convective processes has been developed. Complex spatiotemporal behaviors, including chaos, coherence and patterns, have been addressed. The numerical results show that, in spatial behaviors, the CML model can simulate stochastic interactions not only in weakly but also in strongly coupled cases.

The geomorphologic process has been studied with the CML model to demonstrate that the evolution of sand ripples and dunes on the sand-underlying surface subjected to fluid flow is a combined interaction of the deterministic factors and the stochastic ones. The principle of the geomorphologic change of sand ripples and dunes can be described with the maximal entropy corresponding to equilibrium state and the minimal entropy production rate corresponding to non-equilibrium state. In the numerical examples, the CML model demonstrated the evolution of desert geomorphology, and illustrated the formation of aeolian sand dune. The numerical results are qualitatively in agreement with the field observations in the Sahara Desert, Arabian Desert and Namib Desert, etc.

This study also presents a new approach to predict the evolution of dunes and ripples, explains the solitary phenomena, and especially demonstrates that the nonlinear effect plays an important role in the actual evolution of aeolian ripple.

8. Acknowledgments

Financial supports of the Chongqing Education Foundation (KJ1400324) and Chongqing Natural Science Foundation (CSTC2010 BB7084) and helps of the Henna University are acknowledged. The authors are also thankful to the anonymous reviewers whose suggestions and constructive comments substantially improved our manuscript.

References

1. G.D. DING, *Status and prospect of study on two focuses in aeolian physics*, Journal of Desert Research, **28**:395-398, 2008 [in Chinese].
2. Q.H. ZHANG, T.D. MIAO, *Surface waves in aeolian bedforms*, Physics Letters A, **372**, 3429-3433, 2008.
3. I.K. MCEWAN, B.B. WILLETTS, *On the prediction of bed-load sand transport rate in air*, Sedimentology, **41**, 1241-1251, 1994.
4. P.J. SPIES, I.K. MCEWAN, G. R. BUTTERFIELD, *On wind velocity profile measurements taken in wind tunnels with saltating grains*, Sedimentology, **42**, 515-521, 1995.
5. M. SORENSEN, I.K. MCEWAN, *On the effect of mid-air collisions on aeolian saltation*, Sedimentology, **43**, 65-76, 1996.
6. M.V. CARNEIRO, N.A.M. ARAUJO, T. PAHTZ, H.J. HERRMANN, *Midair collisions enhance saltation*, Physical Review Letters, 111, 058001, 2013.
7. I.K. MCEWAN, *Bagnold's kink: a physical feature of a wind velocity profile modified by blown sand?* Earth Surface Processes and Landforms, **18**, 2, 145-156, 1993.
8. K. PYE, N. LANCASTER, *Aeolian sediments: ancient and modern* (Special publication 16 of the IAS), Blackwell, Oxford, UK, 1993.
9. S.E. COLEMAN, V.I. NIKORA, B.W. MELVILLE *et al.*, *SWAT.nz: New-Zeland-based "Sand Waves and Turbulence" experimental programme*, Acta Geophysica, **56**, 2, 417-439, 2008.
10. S.E. COLEMAN, V.I. NIKORA, *Fluvial dunes: initiation, characterization, flow structure*, Earth Surface Processes and Landforms, **36**, 39-57, 2011.
11. V.I. NIKORA, D.G. GORING, B.J.F. BIGGS, *On gravel-bed roughness characterization*, Water Resources Research, **34**, 517-527, 1998.
12. A. SINGH, M. GUALA, S. LANZONI, E. FOUFOULA-GEORGIU, *Bedform effect on the reorganization of surface and subsurface grain size distribution in gravel bedded channels*, Acta Geophysica, **60**, 1607-1638, 2012.
13. A. SINGH, E. FOUFOULA-GEORGIU, F. PORTÉ-AGEL, P.R. WILCOCK, *Coupled dynamics of the co-evolution of gravel bed topography, flow turbulence and sediment transport in an experimental channel*, Journal of Geophysical Research, **117**, F04016, 2012.
14. K. KANEKO, *Pattern dynamics in spatiotemporal chaos*, Physica D, **34**, 1-41, 1989.
15. M.C. CROSS, P.C. HOHENBERG, *Pattern formation out of equilibrium*, Review Modern Physics, **65**, 851-1112, 1993.

16. J. A. ACEBRÓN, L.L. BONILLA, C.J. PÉREZ VICENTE, F. RITORT, R. SPIGLER, *The Kuramoto model: a simple paradigm for synchronization phenomena*, Review Modern Physics, **77**, 137–185, 2005.
17. J.P. GOLLUB, J.S. LANGER, *Pattern formation in nonequilibrium physics*, Review Modern Physics, **71**, 5396–5403, 1999.
18. G. DANGELMAYR, L. OPREA, *Dynamics and Bifurcation of Patterns in Dissipative Systems*, World Scientific Publishing Press, Singapore, 2004.
19. T. BOHR, M.H. JENSEN, G. PALADIN, A. VULPIANI, *Dynamical Systems Approach to Turbulence*, Cambridge University Press, Cambridge, UK, 1998.
20. T.B. LIVERPOOL, S.F. EDWARDS, *Dynamics of a meandering river*, Physical Review Letters, **75**, 16, 3016–3019, 1995.
21. B.F. EDWARDS, D.H. SMITH, *River meandering dynamics*, Physical Review E, **65**, 4, 046303(1-12), 2008.
22. E. SOMFAI, L.M. SANDER, *Scaling and river networks: a Landau theory for erosion*, Physical Review E, **56**, 1, 1–4, 1997.
23. D.O. MAIONCHI, A.F. MORAIS, R.N. COSTA FILHO, J.S. ANDRADE, JR., H.J. HERRMANN, *Model for erosion-deposition patterns*, Physical Review E, **77**, 061402, 2008.
24. S.G. DE BARTOLO, L. PRIMAVERA, R. GAUDIO, A. D’IPPOLITO, M. VELTRI, *Fixed-mass multifractal analysis of river networks and braided channels*, Physical Review E, **74**, 026101, 2006.
25. A.P. MEHTA, C. REICHHARDT, C.J. OLSON, F. NORI, *Topological invariants in microscopic transport on rough landscapes: morphology, hierarchical structure, and Horton analysis of river-like networks of vortices*, Physical Review Letters, **82**, 18, 3641–3644, 1999.
26. F. ENGELUND, J. FREDSOE, *Sediment ripples and dunes*, Annual Review of Fluid Mechanics, **14**, 13–37, 1982.
27. K. KROY, G. SAUERMAN, H.J. HERRMANN, *Minimal model for aeolian sand dunes*, Physical Review E, **66**, 031302, 2002.
28. H. ELBELRHITI, P. CLAUDIN, B. ANDREOTTI, *Field evidence for surface-wave induced instability of sand dunes*, Nature, **437** (7059), 720–723, 2005.
29. B. ANDREOTTI, P. CLAUDIN, O. POULIQUEN, *Aeolian sand ripples: experimental evidence of fully developed states*, Physical Review Letters, **96**, 028001, 2006.
30. G. SEMINARA, *Fluvial sedimentary patterns*, Annual Review of Fluid Mechanics, **42**, 43–66, 2010.
31. R.J. HUGGETT, *Dissipative systems: implications for geomorphology*, Earth Surface Processes and Landforms, **13**, 1, 45–49, 1988.
32. B. SIVAKUMAR, *Chaos theory in geophysics: past, present and future*, Chaos, Solitons and Fractals, **19**, 2, 441–462, 2004.
33. J.D. PHILLIPS, *Self-organization and landscape evolution*, Progress in Physical Geography, **19**, 3, 309–321, 1995.
34. V.P. SINGH, *Hydrologic synthesis using entropy theory: review*, Journal of Hydrologic Engineering, ASCE, **16**, 421–433, 2011.

35. A.R. VASCONCELLOS, J.G. RAMOS, R. LUZZI, *Ensemble formalism for nonequilibrium systems and an associated irreversible statistical*, Brazilian Journal of Physics, **35**, 689–717, 2005.
36. X.S. XING, *Dynamic statistical information theory*, Science in China: Series G, **49**, 1–37, 2006.
37. B.L. YANG, *Thermodynamics rational reconstruction and dialectic unification of maximum entropy principle and minimum entropy production rate—re-explore “rational principles” in natural science study*, World Science, 40–42, 2003 [in Chinese].
38. R.A. BAGNOLD, *The Physics of Blown Sand and Desert Dunes*, London, Methuen Corporation, UK, 1941.
39. N. CHIEN, Z.H. WAN, *Mechanics of Sediment Transport*, ASCE Press, Reston. USA, 1999.
40. A. FOURRIERE, P. CLAUDIN, B. ANDREOTTI, *Bedforms in a turbulent stream: formation of ripples by primary linear instability and of dunes by nonlinear pattern coarsening*, Journal of Fluid Mechanics, **649**, 287–328, 2010.
41. C. MENDOZA, H.W. SHEN, *Investigation of turbulent flow over dunes*, Journal of Hydraulic Engineering ASCE, **116**, 459–477, 1990.
42. V.D. NIKORA, A.N. SUKHODOLOV, P.M. ROWINSKI, *Statistical sand wave dynamics in one-directional water flows*, Journal of Fluid Mechanics, **351**, 17–39, 1997.
43. S. HA, G.R. DONG, G.Y. WANG, *Morphodynamic study of reticulate dunes at south-eastern fringe of the Tengger Desert*, Science in China (Series D), **42**, 207–215, 1999.
44. S.B. IDSO, *Surface energy balance and the genesis of deserts*, Arch. Met. Geoph. Biokl., Ser. A, **30**, 253–260, 1981.
45. X. WEI, Z.B. LI, *Applicative limitations of sediment transport on predictive modeling in geomorphology*, Journal of Geographical Science, **14**, 94–104, 2004.
46. M. KARPINSKI, R.J. BIALIK, P.M. ROWINSKI, *Application of lattice Boltzmann method for generation of flow velocity field over river bed-forms*, GeoPlanet: Earth and Planetary Sciences, Experimental and Computational Solutions of Hydraulics Problems, P. Rowinski [Ed.], 327–335, 2013.
47. A. MASSELOT, B. CHOPARD, *A lattice Boltzmann model for particle transport and deposition*, Europhysics Letters, **100**, 6, 1–6, 1998.
48. R.J. BIALIK, V.I. NIKORA, P.M. ROWIŃSKI, *3D Lagrangian modelling of saltating particles diffusion in turbulent water flow*, Acta Geophysica, **60**, 6, 1639–1660, 2012.
49. R.J. BIALIK, *Numerical study of near-bed turbulence structures influence on the initiation of saltating grains movement*, Journal of Hydrology and Hydromechanics, **61**, 3, 202–207, 2013.
50. U. FRISCH, *Turbulence*, Cambridge University Press, Cambridge, UK, 1995.
51. G. GAO, *A theory of dissipation and dispersion cooperation of turbulence*, Science in China (Series A), **18**, 616–629, 1985.
52. S.D. LIU, S.K. LIU, *KdV-Burgers equation modeling of turbulence*, Science in China (A), **35**, 576–586, 1992.

-
53. Z.C. LIU, *Study on random and coherence states using a family of CML models*, Chinese Physics B, **18**, 636–645, 2009.
 54. M. PINEDA, M.G. COSENZA, *Synchronization in driven versus autonomous coupled chaotic maps*, Physical Rev. E, **71**, 057201, 2005.
 55. G. FRANCISCO, P. MURUGANANDAM, *Local dimension and finite time prediction in spatiotemporal chaotic systems*, Physical Rev. E, **67**, 066204, 2003.
 56. I.R. ITURBE, M. MARANI, R. RIGON, *Self-organized river basin landscapes: fractal and multifractal characteristics*, Water Resource Research, **30**, 3531–3539, 1994.
 57. M. COLOMBINI, *Revisiting the linear theory of sand dune formation*, Journal of Fluid Mechanics, **502**, 1–16, 2004.
 58. T. STOESSER, C. BRAUN, M. GARCÍA-VILLALBA, W. RODI, *Turbulence structures in flow over two-dimensional dunes*, Journal of Hydraulic Engineering, ASCE, **134**, 42–55, 2008.
 59. P. CLAUDIN, B. ANDREOTTI, *A scaling law for aeolian dunes on Mars, Venus, Earth, and for subaqueous ripples*, Earth Plan. Sci. Lett., **252**, 20–44, 2006.
 60. V. NIKORA, D. GORING, *Spectral scaling in Mars topography: effect of craters*, Acta Geophysica, **54**, 1, 102–112, 2006.
 61. V. NIKORA, D. GORING, *Mars topography: bulk statistics and spectral scaling*, Chaos, Solitons, and Fractals, **19**, 2, 427–439, 2004.

Received December 3, 2013; revised version March 25, 2014.
